arXiv:1701.06251v1 [cond-mat.mtrl-sci] 23 Jan 2017

Insulating titanium oxynitride for visible light photocatalysis

Yuta Aoki,[1,2,3,*] Sinisa Coh,[3,4,5] Steven G. Louie,[3,4] Marvin L. Cohen,[3,4] and Susumu Saito[1,6,7]

[1] *Department of Physics, Tokyo Institute of Technology, 2-12-1 Oh-okayama, Meguro-ku, Tokyo 152-8551, Japan*
[2] *International Education and Research Center of Science, Tokyo Institute of Technology, 2-12-1 Oh-okayama, Meguro-ku, Tokyo 152-8551, Japan*
[3] *Department of Physics, University of California, Berkeley, California 94720, USA*
[4] *Materials Sciences Division, Lawrence Berkeley National Laboratory, Berkeley, California 94720, USA*
[5] *Department of Mechanical Engineering, Materials Science and Engineering, University of California Riverside, Riverside, CA 92521, USA*
[6] *International Research Center for Nanoscience and Quantum Physics, Tokyo Institute of Technology, 2-12-1 Oh-okayama, Meguro-ku, Tokyo 152-8551, Japan*
[7] *Materials Research Center for Element Strategy, Tokyo Institute of Technology, 4259 Nagatsutacho, Midori-ku, Yokohama, Kanagawa 226-8503, Japan*

(Dated: January 24, 2017)

We propose a systematic approach to obtain various forms of insulating titanium oxynitrides $Ti_nN_2O_{2n-3}$ and we conduct a detailed study on its $n = 2$ case, Ti_2N_2O. We study the energetics and the electronic structures of Ti_2N_2O and compare these results with those of pristine and nitrogen-doped TiO_2 within the framework of the density-functional theory (DFT) and the GW approximation. We find that Ti_2N_2O is semiconducting with the calculated band-gap of 1.81 eV, which is significantly smaller than those of pristine TiO_2 rutile (3.14 eV) or anatase (3.55 eV). Furthermore, the reduction of the band-gap of Ti_2N_2O is realized not by lowering of the conduction-band minimum but by rising the valence-band maximum. Therefore the proposed Ti_2N_2O has suitable band-edge alignment for water-splitting photocatalysis. Finally, total energy calculations indicate that Ti_2N_2O is potentially easier to synthesize than nitrogen-doped TiO_2. Based on these results, we propose Ti_2N_2O as a promising visible-light photocatalytic material.

I. INTRODUCTION

Titanium dioxide TiO_2 is extensively studied as a functional material with the potential of being used in various technological applications such as photocatalysis, photovoltaics, and oxide electronics.[1–4] One of the most interesting applications is the photocatalysis of water into hydrogen and oxygen gas.[5–8] However, the experimental optical band gap of TiO_2 is 3.0 eV in rutile and 3.2 eV in anatase phase.[9–14] Therefore pristine TiO_2 is not photoactive under a large part of the solar spectrum.[6,8] However, to improve water splitting efficiency, it is not enough to just reduce the band gap. TiO_2 must maintain appropriate band energy alignment with water oxidation and reduction levels. While the conduction band in TiO_2 is already aligned well with water reduction level, its valence band is too low in energy. In order to optimize the photocatalytic performance, the band-gap reduction in titanium oxide must come from an upward energy shift of the valence band, not from a downward shift of the conduction band.[8,15]

Several methods such as impurity doping and forming solid solutions have been proposed in earlier reports to improve photocatalytic activity of TiO_2 under visible light.[8,16–19] As for the solid-solution method, the TiO_2-ZrO_2 solid solution was reported to have the absorption tail in the visible-light region.[20] Also, the reduction of the band gap was theoretically predicted for the TaON-TiO_2 solution.[21] On the other hand, nitrogen doping was shown to add the absorption tail in the visible-light region by Asahi et al.[22] and this was followed with many other experimental and theoretical studies.[15,23–40] The effectiveness of the nitrogen doping is derived from the fact that atomic $2p$ nitrogen states are higher in energy than atomic $2p$ oxygen states. Therefore nitrogen doping raises the valence band of TiO_2 as it is formed primarily from oxygen $2p$ states.[41,42,44]

However, nitrogen doping into TiO_2 does not give a new peak in the visible-light region. Instead, it just adds a shoulder to the original peak in the ultraviolet region.[23–27] Most likely, this happens because the nitrogen concentration is so small that the absorption via the nitrogen-induced states only occurs around the nitrogen dopants. Therefore, to enhance visible-light absorption with nitrogen doping, it is necessary to increase the nitrogen concentration level. To the best of our knowledge, the highest reported nitrogen concentration in TiO_2 is 15 %.[34] Several studies suggested that oxygen vacancies play a crucial role in stabilizing nitrogen substitution,[45,46] as is expected from the electron-counting rule. Since concentration of oxygen vacancies in native TiO_2 such as rutile or anatase is relatively low, there is a natural limit to the amount of nitrogen one can substitute into TiO_2.

Here we propose an alternative way to achieve much higher nitrogen concentrations in titanium oxide systems. Instead of focusing on TiO_2 stoichiometry with a limited number of native oxygen vacancies, we consider here ordered compounds with composition Ti_nO_{2n-1}, where n

is any positive integer. These systems can be viewed as ordered oxygen-deficient variants of TiO_2 with a large concentration of oxygen vacancies. Since oxygen vacancies stabilize nitrogen substitutions, one can expect that these systems could achieve much higher nitrogen concentrations than TiO_2. The compound with $n = 2$ has the well known corundum structure as its ground state[47–49] while the structures of $n \geq 3$ compounds are known as Magnéli phases.[50–52]

Since the nominal titanium valency in Ti_nO_{2n-1} is less than +IV, one might expect them to be metallic due to partially occupied d-levels on titanium. However, it is found experimentally that corundum Ti_2O_3 and several Magnéli phases exhibit the metal-insulator transition[53–63] with a small charge-ordering gap one or two orders of magnitude less than in TiO_2.[64–66] (The values of the charge-order gap in these systems are between 27 and 250 meV.[54,55,66–72]) Therefore, to achieve large-gap insulating state without charge ordering, one needs to replace two out of $2n-1$ oxygen atoms with nitrogen, thus achieving composition

$$Ti_nN_2O_{2n-3} \quad (n \geq 2)$$

restoring the highly stable +IV valency of titanium. We propose this as a purely insulating titanium oxynitride. It is highly notable that this approach has high controllability over electronic properties since one can tune the nitrogen concentration while keeping the titanium valency +IV by choosing the appropriate value for n.

Nitrogen substitution into Ti_nO_{2n-1} systems was first reported by Hyett and his co-workers for the $n = 3$ case ($Ti_{3-\delta}O_4N$, $0.06 < \delta < 0.25$)[73,74] and later extended to larger n ($5 \leq n \leq 8$) cases by Mikami and Ozaki ($Ti_n(O,N)_{2n-1}$).[75] However, the resistivity of their samples is quite low (10–1000 $\mu\Omega$m). Therefore these samples are likely quite far away from the ideal $Ti_nN_2O_{2n-3}$ configuration. As far as we know, insulating solid material with nominal $Ti_nN_2O_{2n-3}$ configuration has not been synthesized up to now while there is an experimental report on the existence of molecules with the composition Ti_2N_2O, which corresponds to the $n = 2$ case.[76] On the other hand, theoretical prediction of $Ti_nN_2O_{2n-3}$ solid compounds has been done for the $n = 3$ case ($Ti_3N_2O_3$) by Wu and his co-workers via a high throughput screening method within the density functional theory (DFT).[77] They predicted $Ti_3N_2O_3$ based on the structure of Ta_3N_5,[78] which is almost isomorphic to the α-Ti_3O_5 structure. Within the Δ-sol method they obtained the band gap of 2.37 eV with a favorable band-edge position for water splitting.[79]

In this paper, we focus on the oxynitride Ti_2N_2O ($n = 2$ case) with corundum-like structure since it has the highest nitrogen concentration among all $n \geq 2$. However, our conclusions might extend to Magnéli phases ($n \geq 3$) as well. In addition, we study nitrogen-doped TiO_2 so that we can compare the nitrogen substitutional energy and the electronic structure with those of Ti_2N_2O.

II. METHODS

Our electronic-structure calculations are based on the framework of the density-functional theory (DFT).[80,81] We also employ the GW approach[82–84] to compute quasiparticle band structures of pristine TiO_2.

In DFT calculations we use the generalized gradient approximation (GGA)[85] with the Perdew-Burke-Ernzerhof (PBE) exchange-correlation functional.[86] We expand the Kohn-Sham orbitals in plane-wave expansion with the cut-off energy of 200 Ry. We employ the pseudopotential method with the Troullier-Martins norm-conserving pseudopotentials.[87] We generated pseudopotentials for Ti, O, and N with the charged Ti^{4+} and neutral O and N configurations. In generating the pseudopotential for Ti, the $3s$ and $3p$ semicore states are treated as valence states and the cutoff radii for the $3s$, $3p$, and $3d$ states are set to be 0.90 a_B, 0.90 a_B, and 1.00 a_B, respectively, where a_B is the Bohr radius. In generating the pseudopotentials for O and N, the cutoff radii both for the $2s$ and $2p$ states are set to be 1.05 a_B. The k-points sampling is performed using the Monkhorst-Pack method[88] with 4×4×6, 4×4×2, and 6×6×2 grids for the primitive unit cell of rutile TiO_2, and the conventional unit cells of anatase TiO_2 and corundum Ti_2O_3, respectively. For metallic systems, we use the Methfessel-Paxton first-order spreading with the searing of 0.01 Ry in the Brillouin-zone integration.[89] The structural optimization is performed based on the Wentzcovitch damped molecular dynamics.[90] The electronic-structure calculation within the DFT is performed using the Quantum ESPRESSO package.[91]

Quasiparticle band structures are calculated by the one-shot GW approach[82–84] within the generalized plasmon-pole (GPP) model.[92] As the starting point for the one-shot GW calculation, we use the DFT results obtained through the above-mentioned DFT methodology. The number of the calculated bands within the DFT calculation is 1000 per TiO_2 formula unit. The frequency cut-off for the dielectric matrix calculation is set to be 40 Ry. These parameters for the GW calculation were confirmed to give well converged results in a recent GW study for rutile TiO_2.[93] The GW calculation is performed using the BerkeleyGW package.[94]

III. STRUCTURE

In this section, we discuss structural models of nitrogen-substituted TiO_2 and Ti_2O_3 used in our study.

A. Nitrogen substituted TiO_2

Figure 1 shows the crystal structure of pristine rutile and anatase TiO_2, which are representative phases among TiO_2 polymorphs. Rutile has a primitive tetragonal structure with the space group $P4_2/mnm$ (D_{4h}^{14}). Its

unit cell contains two TiO_2 formula units. Anatase has a body-centered tetragonal structure with the space group $I4_1/amd$ (D^{19}_{4h}). Its primitive unit cell also contains only two TiO_2 units.

All oxygen sites in rutile and anatase are crystallographically equivalent. Therefore, there is only one symmetry equivalent way to substitute a single oxygen atom with a nitrogen atom in these structures. In our calculation we replace one out of thirty-two oxygen atoms with nitrogen, both in rutile and anatase phase. After this substitution we fully relax the internal structural coordinates and lattice constants. In the case of rutile this requires a 2×2×2 supercell and in the case of anatase 2×2×1 supercell of its conventional unit cell. These supercells are shown in Fig. 2.

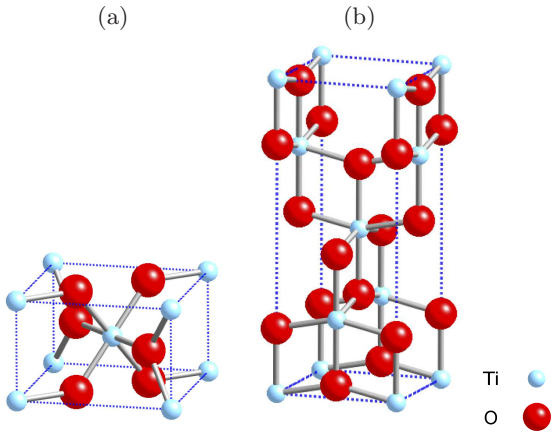

FIG. 1. (Color online) (a): The unit cell of rutile. (b): The conventional unit cell of anatase.

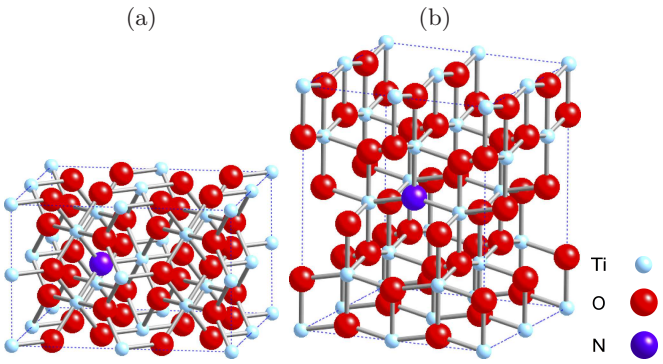

FIG. 2. (Color online) (a): Structural model for nitrogen-doped rutile. One oxygen atom is replaced by one nitrogen atom in the 2×2×2 supercell of rutile. (b): Structural model for nitrogen-doped anatase. One oxygen atom is replaced by one nitrogen atom in the 2×2×1 supercell of the conventional unit cell of anatase.

B. Nitrogen substituted Ti_2O_3: Ti_2N_2O

The crystal structure of corundum Ti_2O_3 is shown in Fig. 3. The corundum structure has rhombohedral symmetry with the space group $R\bar{3}c$ (D^6_{3d}) and its primitive unit cell contains two Ti_2O_3 units.

We use hexagonal conventional unit cell of Ti_2O_3 with twelve titanium and eighteen oxygen atoms as a starting point to obtain structure of titanium oxynitride Ti_2N_2O. We constructed seven representative structural models of Ti_2N_2O by replacing twelve out of eighteen oxygen atoms with nitrogen. Afterwards we relax the structure until it reaches total energy minimum. Seven structures of Ti_2N_2O we considered are shown in Fig. 4 and we label them as Ti_2N_2O-I through Ti_2N_2O-VII in the order of the energetic stability (Ti_2N_2O-I is the most stable). We find that the differences in the formation energy of these seven models are well correlated with the nitrogen and oxygen coordination of titanium atoms. Four out of seven models have all titanium atoms surrounded by four nitrogen and two oxygen atoms. These four models have a very similar calculated total energy (it varies at most 73 meV per Ti_2N_2O formula unit). Remaining three models are significantly less energetically stable (up to 239 meV per Ti_2N_2O formula unit) which we relate to the fact that some of their titanium atoms are surrounded with six nitrogen and no oxygen atoms, as shown in Table I.

TABLE I. Total energy ($E_{\rm tot}$) in meV per Ti_2N_2O formula unit relative to the most stable configuration (model I). We also categorize the titanium atom by its coordination (the numbers of neighboring oxygen and nitrogen atoms) and list the number of each category of titanium atoms in the computational cell. There are twelve titanium atoms per cell in total. The most stable structures (with lowest $E_{\rm tot}$) have all titanium atoms surrounded with four nitrogen and two oxygen atoms. On the other hand, titanium atoms surrounded with six nitrogen and no oxygen atoms are energetically unfavored.

Model	$E_{\rm tot}$	Titanium coordination				
	(meV/Ti_2N_2O)	#N	6	4	3	0
		#O	0	2	3	6
I	0		0	12	0	0
II	21		0	12	0	0
III	21		0	12	0	0
IV	73		0	12	0	0
V	102		4	0	8	0
VI	130		4	0	8	0
VII	239		6	0	4	2

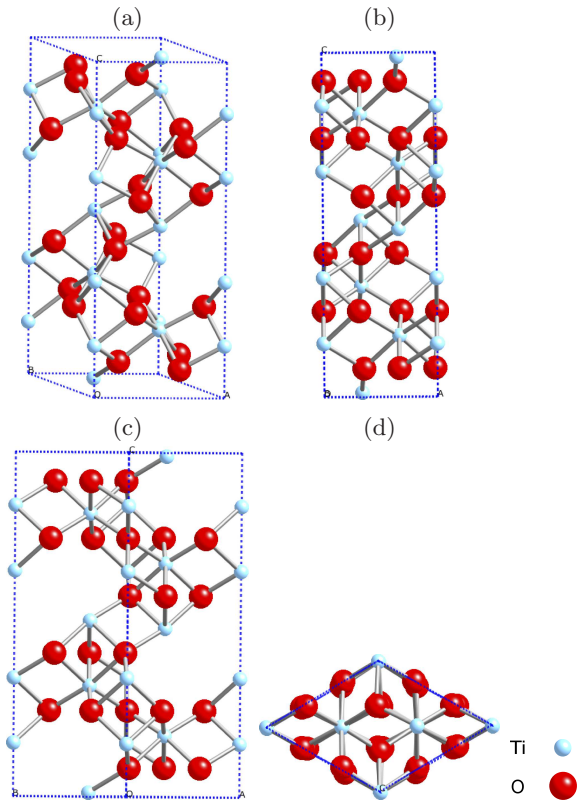

FIG. 3. (Color online) The conventional unit cell of corundum Ti_2O_3 are shown in four ways. (a): Bird-eye view. (b): Projection in the direction of **b**. (c): Projection in the direction of $\mathbf{a}+\mathbf{b}$. (d): Projection in the direction of $-\mathbf{c}$ (top view).

IV. NITROGEN SUBSTITUTION ENERGY

Now we compare energy required to substitute a nitrogen atom into TiO_2 and Ti_2O_3. Since there are no oxygen vancancies in TiO_2 we expect that energy required for substitution in TiO_2 will be significantly larger than that in Ti_2O_3.

We define the substitutional energy E_s per single nitrogen atom in the case of TiO_2 and Ti_2O_3 as,

$$E_s(TiO_2) = E_{tot}(Ti_{16}O_{31}N) - 16E_{tot}(TiO_2) + \frac{1}{2}E_{tot}(O_2) - \frac{1}{2}E_{tot}(N_2) \quad (1)$$

$$E_s(Ti_2O_3) = \frac{1}{2}\left[E_{tot}(Ti_2N_2O) - E_{tot}(Ti_2O_3) + E_{tot}(O_2) - E_{tot}(N_2)\right]. \quad (2)$$

Where $E_{tot}(TiO_2)$ and $E_{tot}(Ti_2O_3)$ are calculated total energies of pristine phases while $E_{tot}(O_2)$ and $E_{tot}(N_2)$ are calculated total energies of molecular oxygen and nitrogen.

Calculated values of substitutional energy E_s are shown in Table II for the cases of TiO_2 and Ti_2O_3. In the case of TiO_2, E_s values are 5.74 eV for the rutile phase and 5.89 eV for the anatase phase. In the case of Ti_2O_3, on the other hand, E_s values are significantly lower, in the range of 3.30–3.42 eV. Therefore, nitrogen substitution into Ti_2O_3 is energetically more favorable than nitrogen doping into TiO_2, as is expected from the titanium valency of +IV in Ti_2N_2O. This result shows that Ti_2N_2O could be created in the laboratory and the existence of Ti_2N_2O molecules[76] also supports this conclusion.

V. ELECTRONIC STRUCTURE

We now discuss its effect on the electronic structure. As is well known, Kohn-Sham energies in the DFT calculation tend to underestimate electronic gaps in most semiconductors.[83,84,95,96] Therefore, we use here GW approximation to obtain improved electron gaps. Since these calculations are rather computationally demanding, we performed them on pristine TiO_2 rutile and anatase and use them to infer GW corrections in nitrogen-substituted cases.

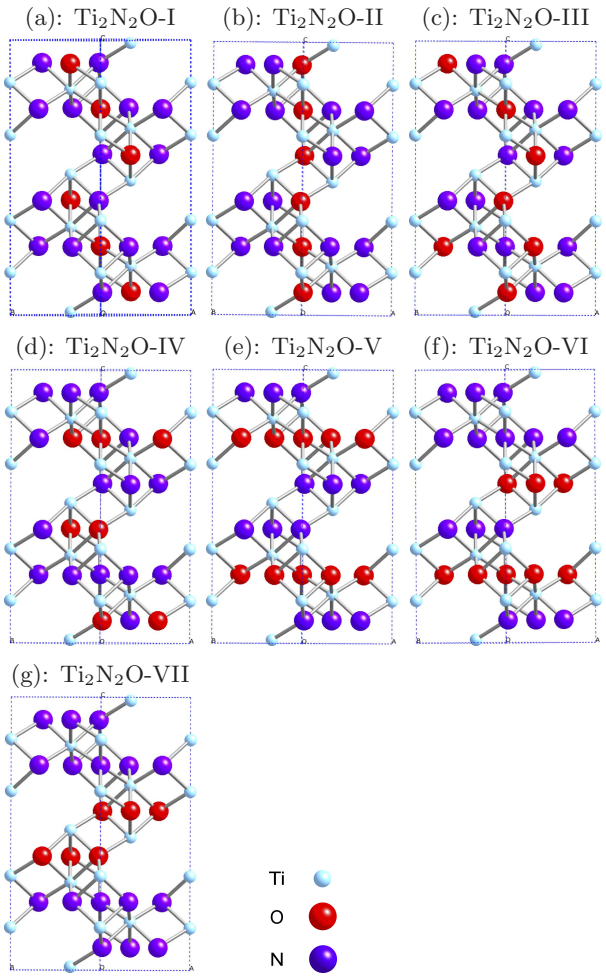

FIG. 4. (Color online) Side views of seven proposed structural models for titanium oxynitride Ti_2N_2O. These figures are projected along the $\mathbf{a}+\mathbf{b}$ direction.

A. Pristine TiO_2 and Ti_2O_3

Figure 5 shows DFT (dashed red line) and GW-corrected (solid blue line) band structures of pristine rutile and anatase TiO_2. We find that the GW-corrected band structure is nearly rigidly opened-up compared to the DFT band structure (scissor-shifted).

We find that the rutile TiO_2 has a direct band gap of 1.87 eV at the Γ point within a DFT calculation. Inclusion of the GW correction changes this direct band gap to 3.19 eV and produces a somewhat smaller indirect Γ-to-R gap of 3.14 eV. This result shows that the scissor-shift due to the GW correction is not completely rigid. Similar result was obtained in a recent GW study as well.[93] Nevertheless, this variation is relatively small.

In the case of anatase TiO_2 we find conduction-band minimum (CBM) at the Γ point but the valence-band maximum (VBM) on the Γ–M line, close to the M point, both in DFT and GW-corrected results. Therefore, the band gap in anatase is indirect. Its magnitude is 2.13 eV within DFT and 3.55 eV with the GW correction.

In the case of pristine Ti_2O_3, we find it to be metallic within the DFT approximation. Therefore, further detailed studies are needed both experimentally and theoretically to discuss the small charge-ordering gap found in previous experiments.[53–58] On the other hand, oxynitride Ti_2N_2O does not possess such difficulty and is insulating with the substantial gap even within DFT as expected from the electron counting argument, which is shown in the following subsection.

Here, we analyze GW corrections to the band gap in pristine rutile and anatase TiO_2. We label GW-corrected and DFT band gaps as E_g^{GW} and E_g^{DFT}, respectively, and define the GW correction to the band gap as $\Delta E_g \equiv E_g^{GW} - E_g^{DFT}$. We plot the ΔE_g with respect to E_g^{DFT} both for rutile and anatase TiO_2 in Fig. 6. As one can see from the figure, two data point for rutile and anatase are almost collinear with the original point, indicating that ΔE_g is approximately proportional to E_g^{DFT} in titanium oxide systems. The proportional trend of the GW correction to the band gap has also been found in the previous literatures.[97–99] Once we assume the proportionality between ΔE_g and E_g^{DFT}, we obtain

$$\Delta E_g \approx 0.67 E_g^{DFT} \tag{3}$$

from the least squares fitting. We use Equation (3) to approximate the scissor-shifts in nitrogen-substituted cases.

B. Nitrogen-substituted cases

Now we are ready to discuss the electronic structure of nitrogen-substituted systems. We list the electron gap, the conduction band maximum (CBM), and the valence band maximum (VBM) calculated based on DFT in Table II for the cases of TiO_2-derived and Ti_2O_3-derived systems. In order to align the energy levels, we use the oxygen 2*s* core level in each system as the reference energy instead of the vacuum level since the calculation of the vacuum level requires detailed analysis of surface conditions. Although energy-level alignment referenced to the oxygen 2*s* level is an approximation, we expect that it works well in this case since it reproduces the rutile/anatase band alignment in pristine TiO_2 both measured by XPS[100] and predicted by DFT[100,101] as well as the band-edge shift induced by nitrogen doping into rutile or anatase predicted in a previous study.[102]

Our results also show that CBM and VBM of anatase are lower than those of rutile by 0.03 eV and 0.45 eV, respectively.

After energy level alignment we introduce the GW scissor-shift correction by adding $\Delta E_g/2$ to CBM and subtracting it from VBM. Therefore total gap is increased by ΔE_g.

Aligned and scissor-shifted energy levels are reported in Table II. We also list the values without the scissor-shifting in the parentheses for references. In the case of

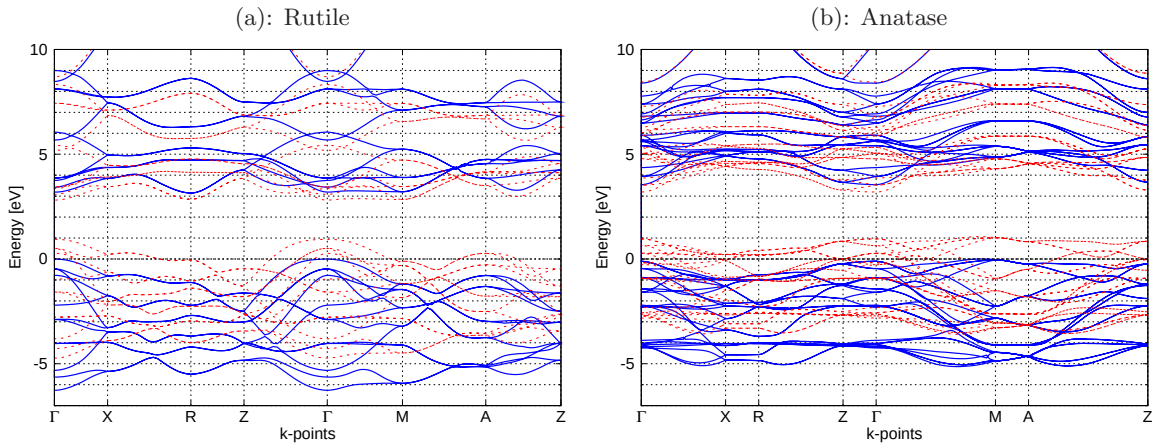

FIG. 5. (Color online) DFT (dashed red line) and GW-corrected (solid blue line) band structures of pristine rutile and anatase. The valence band maximum calculated with GW correction is taken as zero.

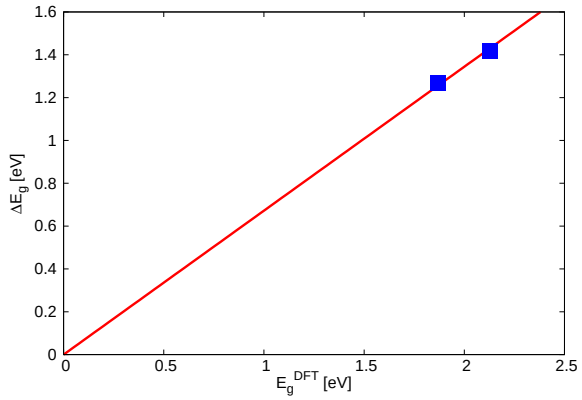

FIG. 6. (Color online) The GW corrections to the band gap, $\Delta E_{\rm g}$, are plotted with respect to the DFT band gap $E_{\rm g}^{\rm DFT}$ both for pristine rutile and anatase.

nitrogen-doped TiO_2, we define the gap as the energy difference between CBM and the Fermi energy (Fermi energy is treated as VBM) since the Fermi energy is on the localized impurity state as discussed later.

Figure 7 compares projected density of states into titanium d, oxygen p, and nitrogen p orbitals together with the total density of states calculated based on DFT. In this figure, energy levels are aligned and both conduction and valence bands are GW scissor-shifted in the same way as in Table II.

We now discuss these results in more detail.

1. *Nitrogen substituted TiO_2*

Substituting nitrogen into either rutile or anatase TiO_2 induces localized states just above the valence band maximum. These localized states are 0.25 eV above valence bands in rutile and 0.20 eV in anatase. In both cases Fermi level is crossing the localized band.

However, nitrogen substitution not only introduces localized states, but also shifts valence and conduction bands relative to the undoped case. As a result, upon nitrogen substitution, the gap of rutile TiO_2 shifts from 3.14 eV to 3.11 eV while the gap of anatase TiO_2 changes from 3.55 eV to 2.98 eV. Similar band-edge shifts are also predicted in a previous DFT study.[102]

As can be seen from Fig. 7 in pristine and nitrogen substituted rutile and anatase TiO_2 the valence band is composed mostly of oxygen p states, while the isolated impurity band is dominated by the nitrogen p states.

2. *Nitrogen substituted Ti_2O_3: Ti_2N_2O*

Now we discuss electronic structure of seven nitrogen-substituted (Ti_2N_2O) models. We find that all seven models are semiconducting as expected from the electron-counting rule.

The calculated band-gap values of Ti_2N_2O models range from 1.81 to 2.32 eV. Among the seven Ti_2N_2O models, Ti_2N_2O-I has the smallest band gap. This model is also energetically the most stable one. The band gap of Ti_2N_2O-I is therefore significantly smaller than that of pristine rutile, anatase, or even nitrogen-doped rutile and anatase. In addition, in Ti_2N_2O, the top of the conduction band is not formed by the localized band as in the case of nitrogen substituted rutile and anatase.

However, as discussed earlier, photocatalytic activity of TiO_2 depends not only on the electronic band gap but it depends also on energy level alignment.

We find that the top of the valence band of the seven Ti_2N_2O models are higher than that of pristine rutile TiO_2 by 0.96–1.76 eV. This alignment is therefore more preferable for water splitting purposes.

Conduction band minimum of most Ti_2N_2O models

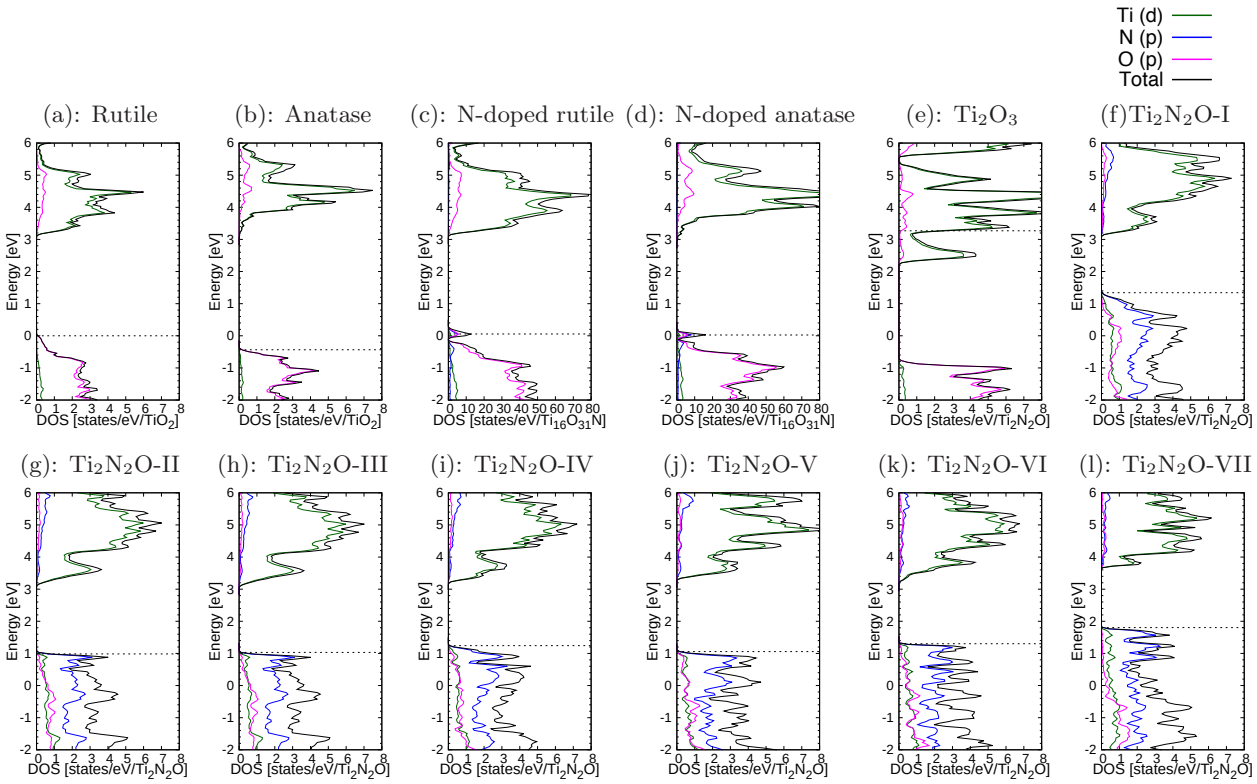

FIG. 7. (Color online) Projected density of states of all systems that we studied. Dotted straight lines indicate VBM (or the Fermi energy for metals). Energy levels are aligned and scissor-shifted as in Table II.

are higher than that of pristine rutile TiO_2. The most stable model (I) had nearly the same conduction band maximum as pristine rutile TiO_2.

Therefore, the reduction of band-gap values in Ti_2N_2O is achieved mostly by the upward shift of VBM, not by the downward shift of CBM. Therefore Ti_2N_2O possesses suitable band-edge position for photocatalytic water decomposition. In all the Ti_2N_2O models, the upper part of the valence band is composed of mainly nitrogen $2p$ states, as shown in Fig. 7. This result shows the effectiveness of nitrogen substitution to shift up the VBM and thus to form a narrower band gap. The amount of band-edge shift in Ti_2N_2O-I, the most stable model, is highly notable because it is the most likely candidate among the seven models. Its VBM and CBM shifts from those of pristine rutile TiO_2 are 1.34 eV and 0.01 eV in the upward direction, respectively.

VI. SUMMARY

In this paper, we have presented a general approach to obtain a variety of purely insulating titanium oxynitride compounds $Ti_nN_2O_{2n-3}$ and we conducted detailed analyses in the cases with the highest nitrogen concentration ($n = 2$). The resulting oxynitride, Ti_2N_2O, is predicted to have suitable band-edge position for photocatalytic water decomposition. Its band gap (1.81 eV) is much smaller in pristine TiO_2 (3.14–3.55 eV). Importantly, most of the band gap reduction originates from the upward shift in energy of the valence band maximum. Furthermore, the energy required to substitute a nitrogen atom into Ti_2O_3 to form Ti_2N_2O is smaller than that into TiO_2. These results show that Ti_2N_2O is a more promising material than nitrogen-doped TiO_2. We hope that this approach would be extended to cases with lower nitrogen concentration and to other transition-metal oxynitrides.

ACKNOWLEDGMENTS

This work was supported from the MEXT Japan Elements Strategy Initiative to Form Core Research Center, JSPS KAKENHI Grant No. JP25107005, and JSPS Grant No. JP14J11856. We also acknowledge the supports by National Science Foundation Grant No. DMR-1508412 (which provided the DFT calculations) and the Theory of Materials Program at the Lawrence Berkeley National Lab funded by the Director, Office of Science, Office of Basic Energy Sciences, Materials Sciences and Engineering Division, U.S. Department of Energy under Contract No. DE-AC02-05CH11231 (which provided the GW calculations). Computational resources have been

provided by the DOE at Lawrence Berkeley National Laboratory's NERSC facility.

* Current address: Center for Materials Research by Information Integration, National Institute for Materials Science, 1-2-1 Sengen, Tsukuba, Ibaraki 305-0047, Japan; AOKI.Yuta@nims.go.jp

[1] F. A. Grant, *Rev. Mod. Phys.* **31**, 646 (1959).
[2] X. Chen and S. S. Mao, *Chem. Rev.* **107**, 2891 (2007).
[3] K. Nakata, T. Ochiai, T. Murakami, and A. Fujishima, *Electrochim. Acta* **84**, 103 (2012).
[4] A. L. Linsebigler, G. Lu, and J. T. Yates, Jr. *Chem. Rev.* **95**, 735 (1995).
[5] A. Fujishima and K. Honda, *Nature* **238**, 37 (1972).
[6] K. Hashimoto, H. Irie, and A. Fujishima, *Jpn. J. Appl. Phys.* **44**, 8269 (2005).
[7] S. S. Mao and S. Shen, *Nature Photonics* **7**, 944 (2013).
[8] M. Ni, M. K. H. Leung, D. Y. C. Leung, and K. Sumathy, *Renew. Sust. Energ. Rev.* **11**, 401 (2007).
[9] J. Pascual, J. Camassel, and H. Mathieu, *Phys. Rev. B* **18**, 5606 (1978).
[10] H. Minoura, M. Nasu, and Y. Takahashi, *Ber. Bunsenges. Phys. Chem.* **89**, 1064 (1985).
[11] H. Tang, H. Berger, P. E. Schmid, F. Lévy, and G. Burri, *Solid State Commun.* **87**, 847 (1993).
[12] H. Tang, K. Prasad, R. Sanjinès, P. E. Schmid, and F. Lévy, *J. Appl. Phys.* **75**, 2042 (1994).
[13] L. Kavan, M. Grätzel, S. E. Gilbert, C. Klemenz, and H. J. Scheel, *J. Am. Chem. Soc.* **118**, 6716 (1996).
[14] N. Hosoka, T. Sekiya, C. Satoko, and S. Kurita, *J. Phys. Soc. Jpn.* **66**, 877-880 (1997).
[15] Y. Aoki and S. Saito, *J. Phys.: Conf. Ser.* **302**, 012034 (2011).
[16] M. Ni, M. K. H. Leung, D. Y. C. Leung, and K. Sumathy, *Renew. Sust. Energy Rev.* **11**, 401 (2007).
[17] A. Zaleska, *Revent Pat. Eng.* **2**, 157 (2008).
[18] B. Viswanathan and K. R. Krishanmurthy, *Int. J. Photoenergy* **2012**, 269654 (2012).
[19] S. Livraghi, M. C. Paganini, E. Giamello, A. Selloni, C. D. Valentin, and G. Pacchioni *J. Am. Chem. Soc.* **128**, 15666 (2006).
[20] Y. Huang, Z. Zheng, Z. Ai, L. Zhang, X. Fan, and Z. Zou, *J. Phys. Chem. B* **110**, 19323 (2006).
[21] W. Dang, H. Chen, N. Umezawa, and J. Zhang, *Phys. Chem. Chem. Phys.* **17**, 17980 (2015).
[22] R. Asahi, T. Morikawa, T. Ohwaki, K. Aoki, and Y. Taga, *Science* **293**, 269 (2001).
[23] T. Morikawa, R. Asahi, T. Ohwaki, K. Aoki, and Y. Taga, *Jpn. J. Appl. Phys.* **40**, L561 (2001).
[24] H. Irie, Y. Watanabe, K. Hashimoto, *J. Phys. Chem. B* **107**, 5483 (2003).
[25] K. Kobayakawa, Y. Murakami, and Y. Sato, *J. Photochem. Photobiol. A: Chem.* **170**, 177 (2005).
[26] P.-G. Wu, C.-H. Ma, and J. K. Shang, *Appl. Phys. A* **8**, 1411 (2005).
[27] G. Yang, Z. Jiang, H. Shi, T. Xiao, and Z. Yan, *J. Mater. Chem.* **20**, 5301 (2010).
[28] T. Lindgren, J. M. Mwabora, E. Avendaño, J. Jonsson, A. Hoel, C.-G. Granqvist, and S.-E. Lindquist, *J. Phys. Chem. B* **107**, 5709 (2003).
[29] G. R. Torres, T. Lindgren, J. Lu, C.-G. Granqvist, and S.-E. Lindguist, *J. Phys. Chem B* **108**, 5995 (2004).
[30] M. Mrowetz, W. Balcerski, A. J. Colussi, and M. R. Hoffmann, *J. Phys. Chem. B* **108**, 17269 (2004).
[31] F. Spadavecchia, G. Cappelletti, S. Ardizzone, M. Ceotto, and L. Falciola, *J. Phys. Chem. C* **115**, 6381 (2011).
[32] Q. Li and J. K. Shang, *J. Am. Ceram. Soc.* **91**, 3167 (2008).
[33] Q. Li and J. K. Shang, *J. Am. Ceram. Soc.* **93**, 3039 (2010).
[34] T. L. Chen, Y. Hirose, T. Hitosugi, and T. Hasegawa, *J. Phys. D: Appl. Phys.* **41**, 062005 (2008).
[35] Y. Nakano, T. Morikawa, T. Ohwaki, and Y. Taga, *Appl. Phys. Lett.* **86**, 132104 (2005).
[36] H. Matsui, H. Tabata, N. Hasuike, H. Harima, and B. Mizobuchi, *J. Appl. Phys.* **97**, 123511 (2005).
[37] M. Kitano, K. Funatsu, M. Matsuoka, M. Ueshima, and M. Anpo, *J. Phys. Chem. B* **110**, 25266 (2006).
[38] C. Burda, Y. Lou, X. Chen, A. C. S. Samia, J. Stout, and J. L. Gole, *Nano Lett.* **3**, 1049 (2003).
[39] J. L. Gole, J. D. Stout, C. Burda, Y. Lou, and X. Chen, *J. Phys. Chem. B* **108**, 1230 (2004).
[40] Y. Aoki and S. Saito, *J. Ceram. Soc. Jpn.* **121**, 373 (2013).
[41] R. Asahi, Y. Taga, W. Mannstadt, A. J. Freeman, *Phys. Rev. B* **61**, 7459 (2000).
[42] S.-D. Mo and W. Y. Ching, *Phys. Rev. B* **51**, 13023 (1995).
[43] K. M. Glassford and J. R. Chelikowsky, *Phys. Rev. B* **45**, 3874 (1992); **46**, 1284 (1992).
[44] H. Nakai, J. Heyd, and G. E. Scuseria, *J. Comput. Chem. Jpn.* **5**, 7 (2006).
[45] M. Batzill, E. H. Morales, U. Diebold, *Phys. Rev. Lett.* **96**, 026103 (2006).
[46] A. K. Rumaiz, J. C. Woicik, E. Cockayne, H. Y. Lin, G. H. Jaffari, and S. I. Shah *Appl. Phys. Lett.* **95**, 262111 (2009).
[47] W. R. Robinson, it J. Solid State Chem. **9**, 255 (1974).
[48] T. J. Godin and J. P. LaFemina, *Phys. Rev. B* **49**, 7691 (1994).
[49] S. V. Ovsyannikov, X. Wu, A. E. Karkin, V. V. Shchennikov, and G. M. Manthilake, *Phys. Rev. B* **86**, 024106 (2012).
[50] S. Andersson and A. Magéli, *Naturwissenschaften* **43**, 495 (1956).
[51] D. Regonini, A. C. E. Dent, C. R. Bowen, S. R. Pennock, J. Taylor, *Mater. Lett.* **65**, 3590 (2011).
[52] D. Regonini, V. Adamaki, C. R. Bowen, S. R. Pennock, J. Taylor, and A. C. E. Dent, *Solid State Ionics* **229**, 38 (2012).
[53] A. D. Pearson, *J. Phys. Chem. Solids* **5**, 316 (1958).
[54] F. J. Morin, *Phys. Rev. Lett.* **3**, 34 (1959).
[55] J. M. Honig and T. B. Reed, *Phys. Rev.* **174**, 1020 (1968).
[56] C. E. Rice and W. R. Robinson, *Mat. Res. Bull.* **11**, 1355 (1976).
[57] I.-H. Hwang, B. Jiang, Z. Jin, C.-I. Park, and S.-W. Han, *J. Appl. Phys.* **119**, 014905 (2016).
[58] M. Imada, A. Fujimori, Y. Tookura, *Rev. Mod. Phys.* **70**, 1039 (1998).

[59] M. Onoda, *J. Solid State Chem.* **136**, 67 (1998).
[60] S. Ohkoshi, Y. Tsunobuchi, T. Matsuda, K. Hashimoto, A. Namai, F. Hakoe, and H. Tokoro, *Nature Chem.* **2**, 539 (2010).
[61] C. Schlenker, S. Lakkis, J. M. D. Coney, and M. Marezio, *Phys. Rev. Lett.* **32**, 1318 (1974).
[62] S. Lakkis, C. Schlenker, B. K. Chakravetry, R. Buder, and M. Marezio, *Phys. Rev. B* **14**, 1429 (1976).
[63] R. F. Bartholomew and D. R. Frankl, *Phys. Rev.* **187**, 828 (1969).
[64] M. Marezio, D. B. McWhan, P. D. Dernier, and J. P. Remeika, *Phys. Rev. Lett.* **28**, 1390 (1972).
[65] M. Abbate, R. Potze, G. A. Sawatzky, C. Schlenker, H. J. Lin, L. H. Tjeng, C. T. Chen, D. Teehan, and T. S. Turner, *Phys. Rev. B* **51**, 10150 (1995).
[66] M. Taguchi, A. Chainani, M. Matsunami, R. Eguchi, Y. Takata, M. Yabashi, K. Tamasaku, Y. Nishino, T. Ishikawa, S. Tsuda, S. Watanabe, C.-T. Chen, Y. Senba, H. Ohashi, K. Fujiwara, Y. Nakamura, H. Takagi, and S. Shin, *Phys. Rev. Lett.* **104**, 106401 (2010).
[67] J. Yahia and H. P. R. Frederikse, *Phys. Rev.* **123**, 1257 (1961).
[68] F. J. Morin, *Bell System Tech. J.* **37**, 1047 (1958).
[69] S. C. Abrahams, *Phys. Rev.* **130**, 2230 (1963).
[70] D. Adler, *Phys. Rev. Lett.* **17**, 139 (1966).
[71] D. Kaplan, C. Schlenker, and J. J. Since, *Philos. Mag.* **36**, 1275 (1977).
[72] K. Kobayashi, T. Susaki, A. Fujimori, T. Tonogai, and H. Takagi, *Europhys. Lett.* **59**, 868 (2002).
[73] G. Hyett, M. A. Green, and I. P. Parkin, *J. Am. Chem. Soc.* **129**, 15541 (2007).
[74] A. Salamat, G. Hyett, R. Q. Cabrera, P. F. McMillan, and I. P. Parkin, *J. Phys. Chem C* **114**, 8546, (2010).
[75] M. Mikami and K. Ozaki, *J. Phys.: Conf. Ser.* **379**, 012006 (2012).
[76] A. Marzouk, H. Bolvin, P. Reinhardt, L. Manceron, J. P. Perchard, B. Tremblay, and M. E. Alikhani, *J. Phys. Chem. A* **118**, 561 (2014).
[77] Y. Wu, P. Lazic, G. Hautier, K. Persson, and G. Ceder, *Energy Environ. Sci.* **6**, 157 (2013).
[78] N. E. Brese, M. O'Keeffe, P. Rauch, and F. J. DiSalvo, *Acta Cryst.* C**47**, 2291 (1991).
[79] M. K. Y. Chan and G. Ceder, *Phys. Rev. Lett.* **105**, 196403 (2010).
[80] P. Hohenberg and W. Kohn, *Phys. Rev.* **136**, B864 (1964).
[81] W. Kohn and L. J. Sham, *Phys. Rev.* **140**, A1133 (1965).
[82] L. Hedin, *Phys. Rev.* **139**, A796 (1965).
[83] M. S. Hybertsen and S. G. Louie, *Phys. Rev. Lett.* **55**, 1418 (1985).
[84] M. S. Hybertsen and S. G. Louie, *Phys. Rev. B* **34**, 5390 (1986).
[85] J. P. Perdew, *Phys. Rev. Lett.* **55**, 1665 (1985).
[86] J. P. Perdew, K. Burke, and M. Ernzerhof, *Phys. Rev. Lett.* **77**, 3865 (1996); *ibid.* **78**, 1396 (1997).
[87] N. Troullier and J. L. Martins, *Phys. Rev. B* **43**, 1993 (1991).
[88] H. J. Monkhorst and J. D. Pack, *Phys. Rev. B* **13**, 5188 (1976).
[89] M. Methfessel and A. T. Paxton, *Phys. Rev. B* **40**, 3616 (1989).
[90] R. M. Wentzcovitch, *Phys. Rev. B* **44**, 2358 (1991).
[91] P. Giannozzi, S. Baroni, N. Bonini, M. Calandra, R. Car, C. Cavazzoni, D. Ceresoli, G. L. Chiarotti, M. Cococcioni, I. Dabo, A. D. Corso, S. de Gironcoli, S. Fabris, G. Fratesi, R. Gebauer, U. Gerstmann, C. Gougoussis, A. Kokalj, M. Lazzeri, L. Martin-Samos, N. Marzari, F. Mauri, R. Mazzarello, S. Paolini, A. Pasquarello, L. Paulatto, C. Sabraccia, S. Scandolo, G. Sclauzero, A. P. Seitsonen, A. Smogunov, P. Umari, and R. M. Wentzcovitch: J. Phys.: Condens. Matter, **21**, 395502 (2009).
[92] S. B. Zhang, D. Tománek, M. L. Cohen, S. G. Louie, and M. S. Hybertsen, *Phys. Rev. B* **40**, 3162 (1989).
[93] A. Malashevich, M. Jain, and S. G. Louie, *Phys. Rev. B* **89**, 075205 (2014).
[94] J. Deslippe, G. Samsonidze, D. A. Strubbe, M. Jain, M. L. Cohen, and S. G. Louie, *Comput. Phys. Commun.* **183**, 1269 (2012).
[95] G. Onida, L. Reining, and A. Rubio, *Rev. Mod. Phys.* **74**, 601 (2002).
[96] S. Kümmel and L. Kronik, *Rev. Mod. Phys.* **80**, 3 (2008).
[97] R. W. Godby, M. Schlüter, and L. J. Sham, *Phys. Rev. B* **37**, 10159 (1988).
[98] S. G. Louie, in *Topics in Computational Materials Science*, edited by C. Y. Fong (World Scientific, Singapore, 1998).
[99] M. van Schilfgaarde, T. Kotani, and S. Faleev, *Phys. Rev. Lett.* **96**, 226402 (2006).
[100] D. O. Scanlon, C. W. Dunnill, J. Buckeridge, S. A. Shevlin, A. J. Logsdail, S. M. Woodley, C. R. A. Catlow, M. J. Powell, R. G. Palgrave, I. P. Parkin, G. W. Watson, T. W. Keal, P. Sherwood, A. Walsh, and A. A. Sokol, *Nature Mater.* **12**, 798 (2013).
[101] P. Deák, B. Aradi, and T. Frauenheim, *J. Phys. Chem. C* **115**, 3443 (2011).
[102] C. DiValentin, G. Pacchioni, and A. Selloni, *Phys. Rev. B* **70**, 085116 (2004).

TABLE II. Summary of results for a conventional substitution of nitrogen into TiO_2 as well as substitution of nitrogen into Ti_2O_3 forming oxynitride Ti_2N_2O. We show substitutional energy per single nitrogen atom E_s, electron gap, conduction band minimum (CBM) and valence band maximum (VBM). CBM and VBM are aligned in energy by using the oxygen $2s$ core level in each system as a reference. After aligning the energy levels, we introduce the scissor-shift by adding $\Delta E_g/2$ to CBM and subtracting it from VBM. ΔE_g is obtained from the GW calculation in pristine cases and is approximated by Eq. (3) in nitrogen-substituted cases. Values without scissor-shifts are listed in the parentheses as a reference. For both values with and without scissor-shift, we take VBM of pristine rutile as zero in energy. Parent Ti_2O_3 phase is metallic within DFT so we only list in the Table location of the Fermi level (within DFT and without scissor-shift).

	E_s (eV)	Gap (eV)	CBM (eV)	VBM (eV)
Pristine TiO_2				
Rutile		3.14	3.14	0.00
		(1.87)	(1.87)	(0.00)
Anatase		3.55	3.11	−0.45
		(2.13)	(1.76)	(−0.37)
TiO_2 with 1/32 N substitution				
Rutile	5.74	3.11	3.17	0.06
		(1.86)	(1.91)	(0.05)
Anatase	5.89	2.98	3.00	0.03
		(1.78)	(1.77)	(−0.01)
Pristine Ti_2O_3				
		Fermi level at 3.27 eV		
Ti_2N_2O oxynitride				
I	3.30	1.81	3.15	1.34
		(1.08)	(2.15)	(1.07)
II	3.31	2.19	3.16	0.96
		(1.31)	(2.08)	(0.77)
III	3.31	2.11	3.12	1.01
		(1.26)	(2.06)	(0.80)
IV	3.34	2.06	3.28	1.22
		(1.23)	(2.23)	(1.00)
V	3.35	2.32	3.35	1.03
		(1.39)	(2.25)	(0.86)
VI	3.37	2.01	3.26	1.25
		(1.20)	(2.22)	(1.02)
VII	3.42	1.99	3.74	1.76
		(1.19)	(2.71)	(1.52)